



REGULAR ARTICLE

Coercivity Enhancement of Pt/Co and Pt/Co/Pt/Co Thin Films by Ar⁺ Ion Irradiation Followed by Heat Treatment

A. Orlov^{1,*} , R. Pedan¹, I. Kruhlov¹, Y. Yavorskyi¹, O. Palchekovskyi¹, O. Dubikovskiyi^{1,2}, O. Kosulya², A. Bodnaruk^{1,3}, I. Vladymyrskiyi¹

¹ National Technical University of Ukraine "Igor Sikorsky Kyiv Polytechnic Institute", 03056 Kyiv, Ukraine

² V. Lashkaryov Institute of Semiconductor Physics, National Academy of Sciences of Ukraine, 03680 Kyiv, Ukraine

³ Institute of Physics, National Academy of Sciences of Ukraine, 03028 Kyiv, Ukraine

(Received 08 August 2025; revised manuscript received 15 December 2025; published online 19 December 2025)

This paper discusses the effect of Ar⁺ ion irradiation followed by thermal annealing on the magnetic and structural properties of Pt/Co and Pt/Co/Pt/Co film stacks as a function of ion bombardment fluence. The correlation between phase formation, chemical depth distribution of the main components, and structure modification related to the change in coercivity has been investigated by the XRD, SIMS, and VSM analysis. We observed a considerable increase in coercivity up to 532 Oe in the four-layered stack after ion pre-irradiation with a fluence of 1×10^{14} ions/cm² and subsequent annealing at 550 °C. The observed enhancement of coercivity is accompanied by local structure disorder with Co and Pt atom displacements and defect clustering, which is enhanced with the increase of the interface number. These results are in good agreement with the depth profile evaluated independently by SRIM simulations.

Keywords: Magnetic thin films, Ion irradiation, Intermixing, Co-Pt alloy, Interface, Phase formation.

DOI: [10.21272/jnep.17\(6\).06001](https://doi.org/10.21272/jnep.17(6).06001)

PACS numbers: 75.70.Cn, 61.72.y

1. INTRODUCTION

Ion irradiation of Co/Pt multilayers is a powerful technique for adjusting and tuning their magnetic properties considerably [1]. These materials are promising for magnetic tunnel junction applications [2] and high-density hard disk drives [3] due to their large coercivity [4]. Investigations of the past decades showed the active use of different types of heavy (Ar⁺ [5], Ga⁺ [6, 7], Kr⁺ [8], Xe⁺ [9]) and light (N⁺ [10, 11], He⁺ [12], and O⁺ [13]) ions, ion energy ranges (from 10 – 30 keV to 2 MeV), and fluence that provide a wide variety of structure modifications.

Normally, to modify structural and magnetic properties of Co/Pt thin films, an additional thermal treatment is required [14] due to the quite slow kinetics of homogenization in the Co-Pt system. The annealing temperature required to induce atomic rearrangement in the CoPt system is relatively high (> 700 °C), which also results in substantial grain growth, which is undesirable for high-density recording [15]. From this point of view, the interdiffusion can be enhanced significantly by the ion-induced generation of additional defects and intrinsic strains at room temperature [16, 17]. Numerous studies have reported [18, 19] that Ar⁺ ion irradiation is an efficient technique for modifying the coercivity of Co/Pt multilayered films by the nearest-neighbor coupling and ballistic ion-mixing mechanisms. This can be explained primarily by modifying the interface quality and inducing intermixing between the Co and Pt layers, as a result of collision-induced intermixing. Ghosh et al.

[20] have reported that the Ar⁺ ion-induced CoPt ordered/disordered phase formation leads to the enhancement in the coercivity, which is more pronounced at higher temperatures. Chang et al. [5] have reported the possibility of formation of a partially ordered (face-centered-tetragonal) CoPt phase with increasing Ar⁺ ion fluence. Kumar et al. [21] have reported that the Ar⁺ ion implantation leads to a reduced exchange coupling in Co₈₀Pt₂₀ thin films. On the other hand, Balk et al. [22] showed the possibility of tuning the Dzyaloshinskii-Moriya interaction in Pt/Co/Pt tri-layers by adjusting the Ar⁺ irradiation around 100 eV without raising coercivity. Maziewski et al. [23] proposed that irradiation-induced changes in the magnetic properties of Pt/Co/Pt stacks are governed by the intermixing of metals along interfaces and the formation of an ordered CoPt alloy phase with high magnetic anisotropy.

Another promising approach for structure and magnetic properties modification is ion irradiation at elevated temperatures or the combination of ion irradiation and heat treatment. As was mentioned earlier, when irradiation and heat treatment are conducted in separate stages, irradiation-induced lattice defects, atomic displacements, and implantation effects may influence the intermixing of Co and Pt during post-annealing. However, the full structural aspects of lattice distortion and their impact on the coercivity upon Ar⁺ ion irradiation in multilayered structures compared to bi-layered stacks, as well as subsequent heat treatment, have not been well studied. On the basis of our earlier investigations of

* Correspondence e-mail: orlov@kpm.kpi.ua



the effect of two type of ions (N^+ and Ar^+) on the evolution of the structural, chemical, and magnetic properties of Co/Pt and Pt/Co heterostructures [24], in which magnetic properties were determined as a function of both layers' arrangement and ion fluence of 110 keV Ar^+/N^+ irradiation, in the present study, the number of Co/Pt interfaces was 3 times increased.

Therefore, the goal of this work is to investigate the correlation between phase formation, chemical depth distribution of the main components, and structure modification related to the change in coercivity of Pt/Co and Pt/Co/Pt/Co stacks upon Ar^+ ion irradiation as a function of fluence and post-annealing in vacuum. Ar^+ ions have been chosen for their wide range of applications in different technological processes. This work provides a deeper insight into the ion-induced stimulation of the coercivity increase that is of particular importance for spintronic applications.

2. MATERIALS AND METHODS OF RESEARCH

2.1 Materials

Function of the ion bombardment fluence, all experimental conditions have been reproduced according to our previous work [24]. Two different film configurations, Pt(10 nm)/Co(10 nm)/substrate bi-layered and Pt(5 nm)/Co(5 nm)/Pt(5 nm)/Co(5 nm)/substrate four-layered stacks, were prepared on $SiO_2/Si(001)$ substrates using magnetron sputtering at room temperature. Before the deposition, silicon substrates were subjected to the standard RCA cleaning procedure. The vacuum chamber was maintained at a background pressure of 5×10^{-8} mbar, with an Ar sputtering pressure set to 8×10^{-4} mbar during deposition. The stacks were fabricated using DC magnetron sputtering for Co and RF for Pt, employing two high-purity (99.9 %) targets, with deposition rates of 2 Å/s and 1.5 Å/s for Co and Pt, respectively.

After deposition, the samples underwent ion pre-irradiation using Ar^+ ions from a Balzers MPB 202 ion implantation system. The ion energy was set at 110 keV, with irradiation fluences of 1×10^{14} ions/cm², 5×10^{14} ions/cm², and 1×10^{15} ions/cm². Pre-irradiated

stacks were annealed in a vacuum of 10^{-6} mbar at 550 °C for 30 minutes. For comparison, non-irradiated samples subjected to the same annealing process were also analyzed. The schematic illustration of the experimental algorithm is shown in Fig. 1. Ar^+ concentration depth profiles were simulated using the SRIM-2013 code applying the Kinchin-Pease formalism. Bi-layered and four-layered stacks were simulated as alternating layers of Pt and Co on a SiO_2 substrate. The densities of each element corresponded to their bulk values. The calculations assumed normal incidence (0°) and used 20000 ions for statistical reliability.

2.2 Methods of Research

The structural and phase compositions of the bi-layered and four-layered stacks after deposition, ion irradiation, and post-annealing were examined using X-ray diffraction (XRD) with a Rigaku Ultima IV diffractometer, utilizing $CuK\alpha$ radiation in θ - 2θ Bragg-Brentano geometry in 2θ range 35°–55° with a step of 0.02° per 2 s at an operating voltage of 30 kV and current of 20 mA. The chemical depth distribution of the main components in the studied film stacks was utilized by secondary ion mass spectrometry (SIMS) technique, using an Ion ToF IV device, applying a beam of primary 2 keV Cs⁺ ions. The changes in coercivity and saturation magnetization were analyzed at room temperature, using the vibrating sample magnetometry (VSM) technique at in-plane and out-of-plane magnetic fields up to 1 kOe.

3. RESULTS AND DISCUSSION

3.1 Structural Characterization and Chemical Depth Profiling

Figure 2 illustrates the XRD patterns of the bi-layered stack after deposition and ion pre-irradiation using Ar^+ ions with varying fluence. After deposition (Fig. 2a), the XRD scan of the bi-layered stack is characterized by the presence of the fundamental fcc-Pt(111) diffraction peak at 39.8° 2θ angular position, lattice constant $a = 3.92$ Å.

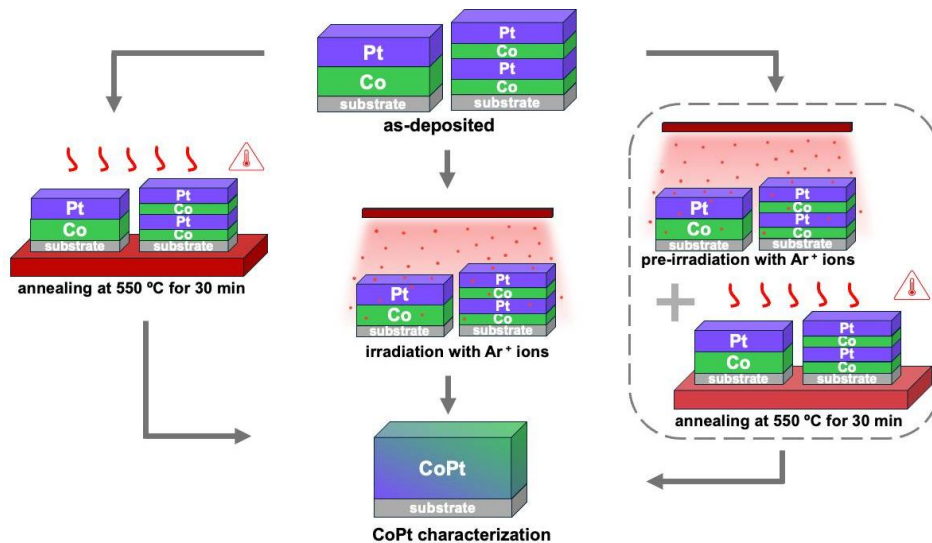


Fig. 1 – The schematic illustration of the treatment regimes used for modification of magnetic and structural properties of bi-layered Pt/Co and four-layered Pt/Co/Pt/Co stacks

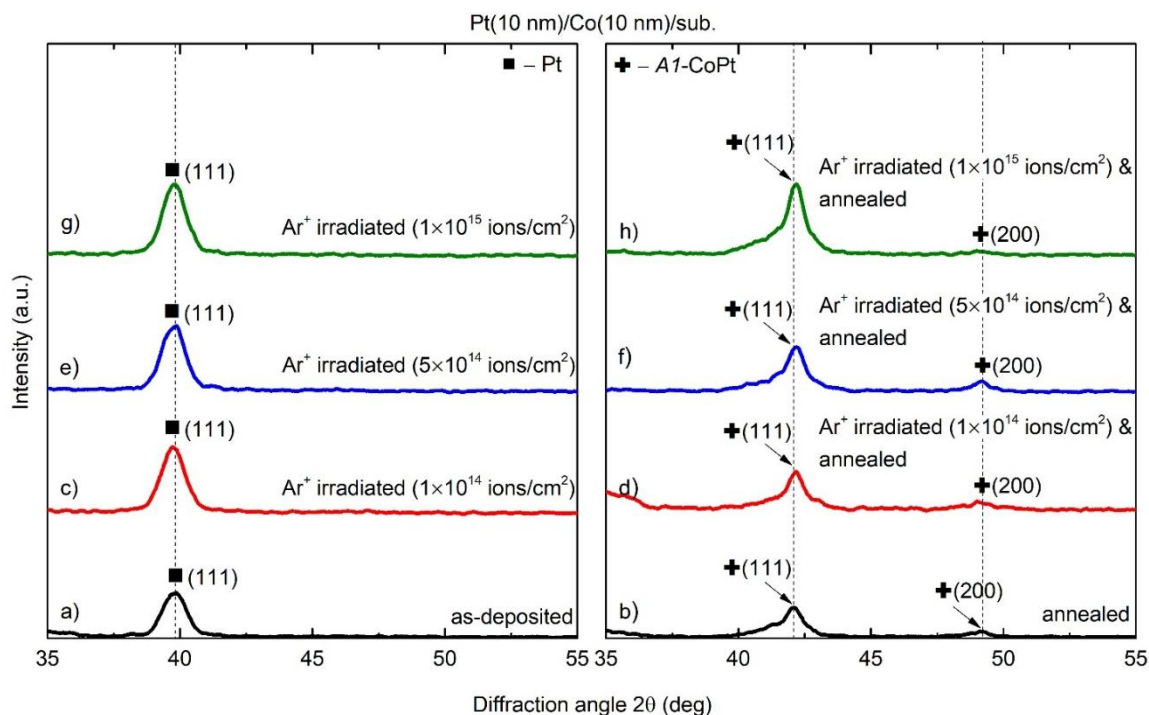


Fig. 2 – XRD patterns of the bi-layered Pt/Co stack after deposition (a), Ar⁺ ion irradiation (c, e, g), single-stage annealing (b), and pre-irradiation followed by post-annealing (d, f, h)

The fundamental *hcp*-Co(101) peak is not observed, which is related to the low atomic scattering factor and low fluorescence yield of Co in CuK α radiation. Pre-irradiation does not lead to structural changes, even with a fluence increase (Fig. 2c, e, g). The lattice constant *a* after bombardment at a fluence of 1×10^{14} ions/cm² is raised to 3.93 Å, while at higher fluence, the lattice constant remains unchanged at the value of 3.92 Å. Both in the as-deposited and in the pre-irradiated stacks with elevated fluence, only the *fcc*-Pt(111) peak is observed. At the same time, post-annealing of bi-layered stacks results in structural modifications with the formation of the disordered A1 CoPt phase, which provides corresponding CoPt(111) and CoPt(200) diffraction peaks plotted at 2θ positions of 42.08° and 49.16°, respectively (Fig. 2b). The A1 CoPt phase lattice constant after single-stage annealing is 3.71 Å. The combination of ion pre-irradiation and post-annealing process does not lead to significant structural changes, in particular, the lattice constant does not change regardless of the fluence (Fig. 2d, f, h). The XRD patterns reveal the same set of diffraction peaks – CoPt(111) and CoPt(200), respectively. The only difference with the elevation of ion fluence is manifested in an increase of CoPt(111) peak intensity with simultaneous broadening of CoPt(200) reflex (Fig. 2h). This observation suggests the presence of a strong preferred orientation along the [111] direction.

Figure 3 shows the XRD patterns of the four-layered stack after deposition and pre-irradiation using Ar⁺ ions with varying fluence. Already after deposition, the film stack demonstrates a significant difference in phase composition compared to the bi-layered stacks. Figure 3a shows that the four-layered stack consists of the *fcc*-Pt, *fcc*-L1₂-CoPt₃, and Co-Pt solid solution phases, providing corresponding fundamental (111) peaks with 2θ angle positions of 39.76°, 40.56°, and 38.84°,

respectively. The calculated from (111) diffraction peak lattice constants are 3.92 Å (for Pt), 3.85 Å (for L1₂-CoPt₃), and 4.01 Å (for Co-Pt solid solution). In the work [6], the formation possibility of the Co-Pt(*fcc*) solid solution during ion irradiation of the sandwich-type Pt(*fcc*)/Co(*hcp*)/Pt(*fcc*) film structure has been demonstrated. Also, Lišková et al. [25] have reported that Co_xPt_{1-x} alloy with variable compositions, defects, and strains can be formed even during the Ar⁺ ion-induced sputtering process. Ion irradiation leads to roughened interfaces and activates interdiffusion between Pt and Co atoms, enhanced by hybridization between the *d*-electrons of Co and Pt. Similarly to the previous case, the fundamental *hcp*-Co(101) peak is not observed. Pre-irradiation does not lead to significant structure changes, even with a fluence increase (Fig. 3c, e, g). Only the ion pre-irradiation at a fluence of 1×10^{14} ions/cm² results in a slight increase of the Pt lattice constant up to 3.94 Å. In both the as-deposited and the pre-irradiated stacks subjected to elevated fluence, solely the *fcc*-Pt(111) diffraction peak is detected. Simultaneously, post-annealing of the bi-layered stacks induces structural transformations, leading to the formation of the disordered A1-CoPt phase, as evidenced by the appearance of CoPt(111) and CoPt(200) diffraction peaks located at 2θ positions of 41.8° and 48.8°, respectively (Fig. 3b). The combined application of ion pre-irradiation and subsequent annealing does not result in substantial structural alterations (Fig. 3d, f, h). The XRD patterns exhibit the same set of diffraction peaks, corresponding to CoPt(111) and CoPt(200), respectively. The sole observed difference at a fluence of 1×10^{14} ions/cm² is an increase in the lattice parameter of the A1-CoPt phase, reaching a value of 3.74 Å.

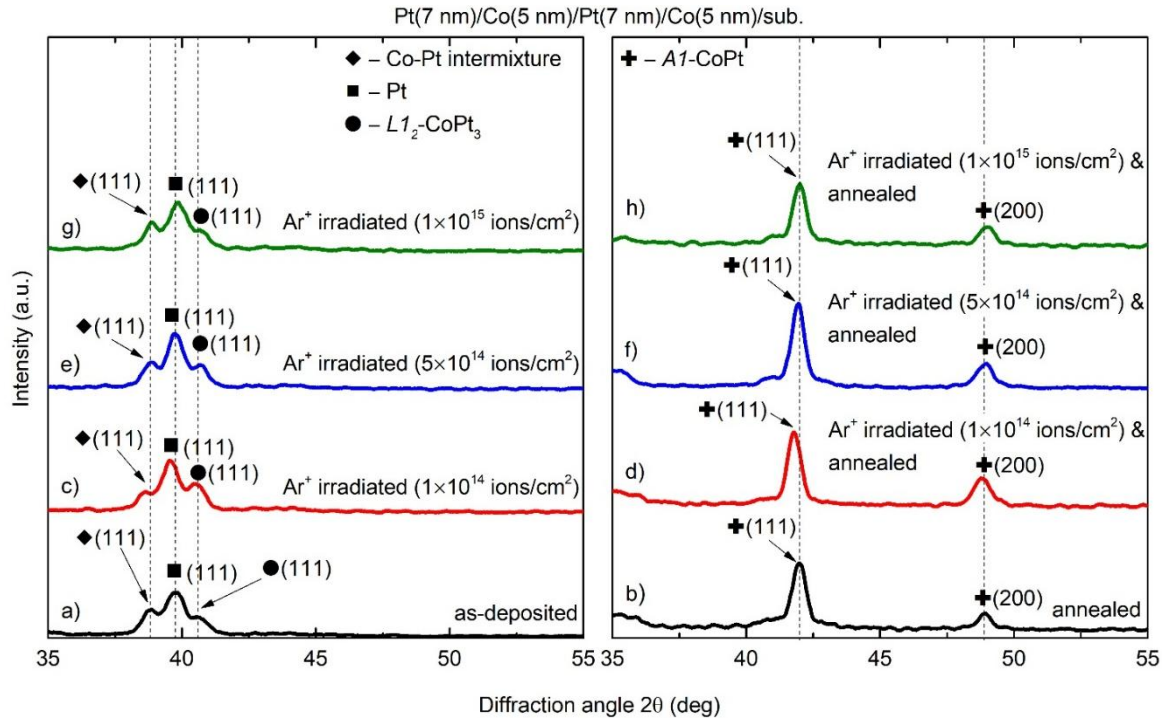


Fig. 3 – XRD patterns of the four-layered Pt/Co/Pt/Co stack after deposition (a), Ar⁺ ion irradiation (c, e, g), single-stage annealing (b), and pre-irradiation followed by the post-annealing (d, f, h)

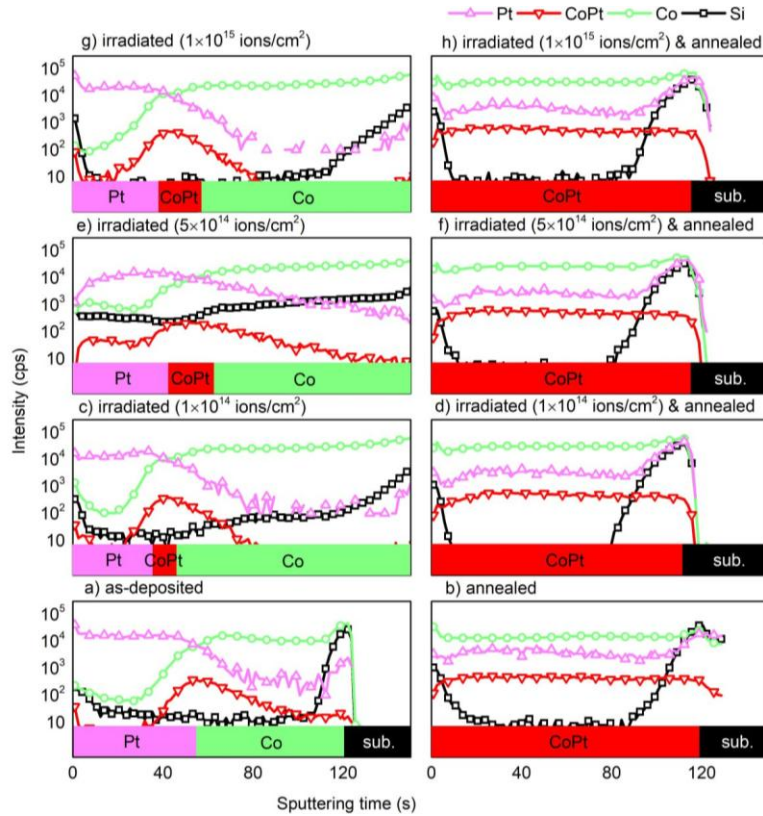


Fig. 4 – SIMS chemical depth profiles of the bi-layered Pt/Co stack after deposition (a), Ar⁺ ion irradiation (c, e, g), single-stage annealing (b), and irradiation followed by the post-annealing (d, f, h). Pt peak intensity was normalized to the total secondary ions' intensity

Secondary ion mass spectrometry (SIMS) was employed to qualitatively assess the interlayer intermixing of Co, Pt, and Si throughout the film thickness. Figure 4 presents the SIMS depth profiles for the bi-layered Pt/Co stack following various processing stages: initial deposition, Ar⁺ ion irradiation, thermal annealing, and sequential irradiation followed by annealing. In the as-deposited state (Fig. 4a), the stack exhibits distinct Co and Pt layers, indicative of well-defined interfaces. However, a moderate interface broadening is observed, accompanied by the emergence of a pronounced signal from complex CoPt secondary ions. The elevated Si signal near the film surface is identified as a hydrocarbon species.

Thermal annealing promotes elemental interdiffusion, leading to a homogenized distribution of Co and Pt

throughout the film (Fig. 4b). Notably, similar Co and Pt depth profiles are detected in the irradiated samples across all three tested fluence levels, indicating that irradiation alone does not drastically alter elemental distribution. However, post-annealing of the irradiated stacks (Fig. 4d, f, h) results in enhanced interdiffusion, as evidenced by the mutual penetration of Co and Pt signals and the overall profile flattening, consistent with diffusion-driven homogenization at 550 °C. At the highest fluence of 1×10^{15} ions/cm² (Fig. 4h), intermixing becomes more pronounced: Co atoms penetrate deeply into the Pt overlayer, while Pt atoms diffuse into the Co layer and tend to segregate near the substrate interface, indicating a strong fluence-dependent enhancement of atomic mobility and redistribution.

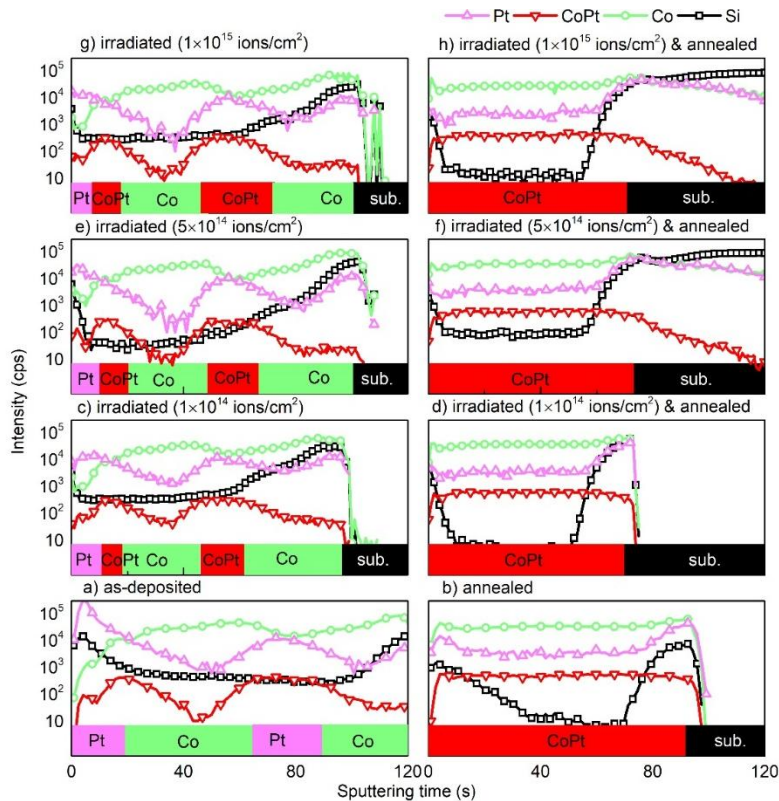


Fig. 5 – SIMS chemical depth profiles of the four-layered Pt/Co/Pt/Co stack after deposition (a), Ar⁺ ion irradiation (c, e, g), single-stage annealing (b), and irradiation followed by the post-annealing (d, f, h). Pt peak intensity was normalized to the total secondary ions' intensities' intensity

Figure 5 illustrates the chemical depth profiles of Pt and Co in the four-layered Pt/Co/Pt/Co stack subjected to various treatment regimes, including Ar⁺ ion irradiation, single-step annealing, and sequential irradiation followed by annealing. In the as-deposited state (Fig. 5a), well-defined interfaces are not observed across the entire stack. Only the upper Pt/Co bilayer exhibits partial modulation, while the lower Pt/Co interface appears significantly intermixed. This is indicated by the emergence of a CoPt complex ion signal and an intensified CoPt peak localized within the Pt layer, suggesting Co diffusion into Pt. These findings are consistent with the XRD results (Fig. 3a) and confirm the formation of the Co-Pt(*fcc*) solid solution. Since Pt and Co are transition metals with partially filled *d*-orbitals, the observed intermixing may be attributed to hybridization between Co 3*d* and Pt 5*d* orbitals. This

hybridization can lower the system's total energy (contributes to the negative enthalpy of mixing), promoting atomic mixing at interfaces, especially at elevated temperatures or under irradiation. Post-annealing (Fig. 5b) results in a complete and uniform intermixing of Pt and Co throughout the film thickness. In contrast, ion irradiation alone, across various fluences (Fig. 5c, e, g), induces only limited redistribution of elements, with the layered architecture remaining largely preserved, even at the highest fluence. Notably, the two-step treatment combining ion pre-irradiation with subsequent annealing (Fig. 5d, f, h) produces a homogeneous elemental distribution, indicating that this approach is more effective in promoting interdiffusion and achieving structural uniformity within the multilayer stack.

3.2 Magnetic Characterization

The evolution of the M - H hysteresis loops (Figs. 5 and 6) further supports structural phase transformations and alloy formation resulting from the ion pre-irradiation followed by thermal annealing. Magnetic hysteresis loop analysis of the films before and after post-deposition treatments indicates the presence of in-plane magnetic anisotropy, primarily attributed to shape anisotropy. In the as-deposited state, the coercivity (H_c) and saturation magnetization (M_s) were measured to be 9 Oe and

549 emu/cc, respectively (Fig. 6a). Following thermal annealing (Fig. 6b) led to an increase in H_c to 296 Oe, which suggests the formation of the ferromagnetic A1-CoPt phase. Meanwhile, M_s has slightly increased to 646 emu/cc. Film stacks after ion irradiation exhibit a negligible change in H_c and M_s , indicating limited structural modifications. It is observed that the coercivity does not increase significantly with increasing irradiation dose; the value lies within the limits from 176 Oe to 183 Oe, and is due to the more uniform structure.

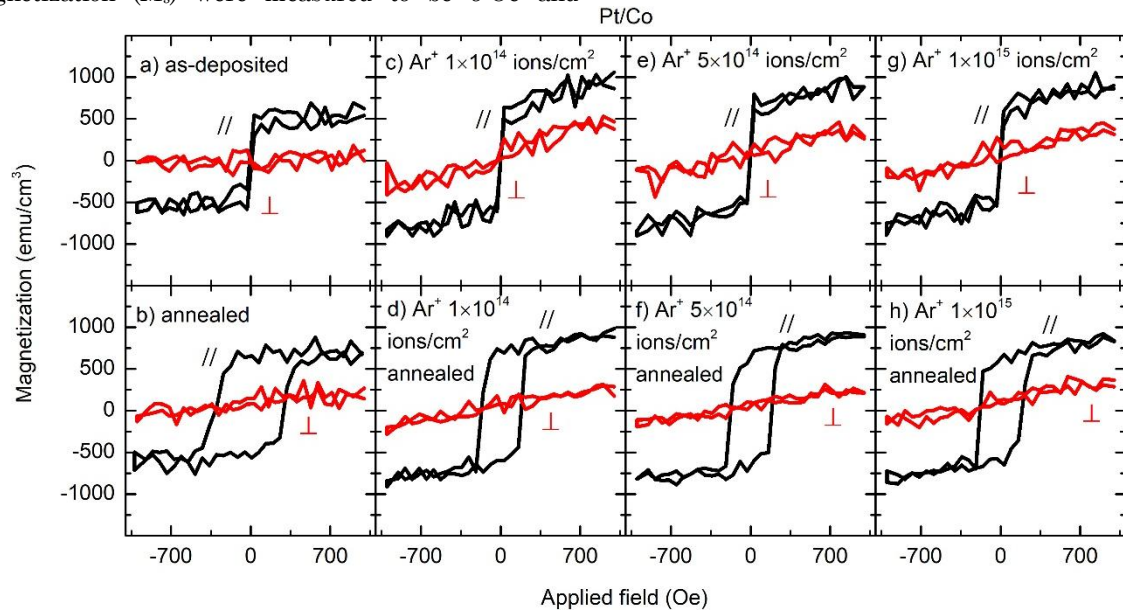


Fig. 6 – M - H hysteresis loops of the bi-layered Pt/Co stack after deposition (a), Ar^+ ion irradiation (c, e, g), single-stage annealing (b), and pre-irradiation followed by the post-annealing (d, f, h)

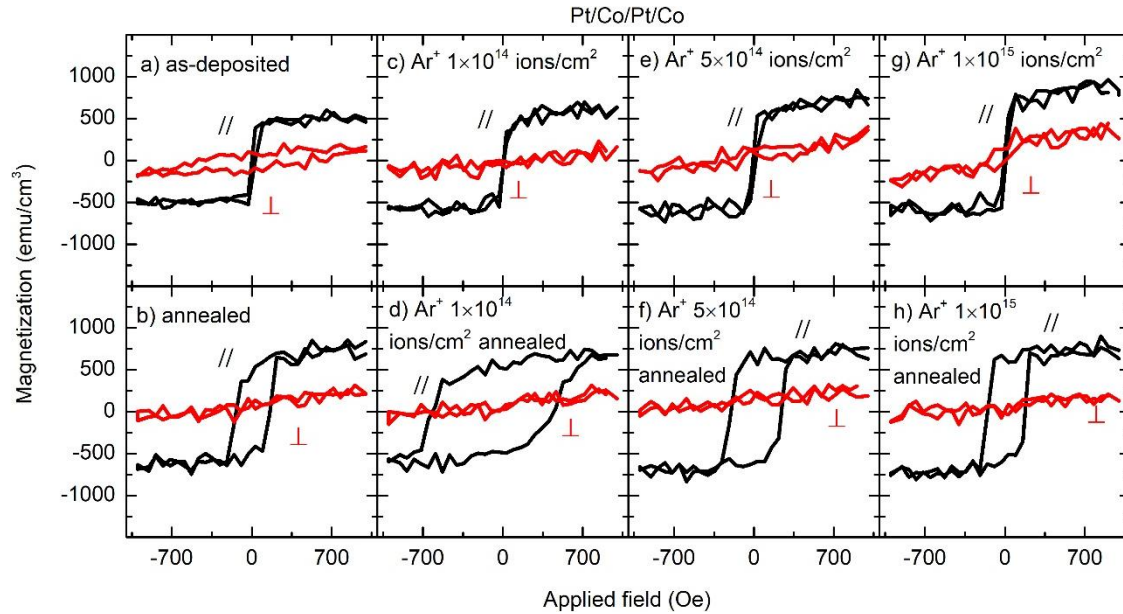


Fig. 7 – M - H hysteresis loops of the four-layered Pt/Co/Pt/Co stack after deposition (a), Ar^+ ion irradiation (c, e, g), single-stage annealing (b), and pre-irradiation followed by the post-annealing (d, f, h)

Figure 7 presents the magnetic hysteresis loops (M - H) of the four-layer stack subjected to Ar^+ ion irradiation, single-step annealing, and a combined sequence of pre-irradiation followed by annealing. In the as-deposited condition (Fig. 7a) and after Ar^+ ion irradiation at different fluences (Fig. 7c, e, g), the linear increase of M_s is observed, and the magnetic behavior remains comparable to that of the bi-layered reference structure. By contrast, single-stage annealing results in a lower coercivity of 148 Oe (Fig. 7b), which is likely associated with partial intermixing occurring during the deposition process and the formation of the soft magnetic CoPt_3 phase. A distinct modification of the magnetic response becomes apparent only when ion irradiation is followed by thermal annealing. The significant rise of H_c up to 532 Oe at fluence 1×10^{14} ions/cm² is observed (Fig. 8). H_c remains higher compared to a bi-layered stack across the same fluence range. In this case, the progressive decrease in coercivity is observed, from 221 Oe to 167 Oe. These results are not visible in the hysteresis loops of a

bi-layered stack due to the lower exchange coupling between the grains.

The considerable increase in coercivity after ion irradiation followed by thermal annealing is attributed to the exchange decoupling between magnetic grains, due to the inhomogeneity of the film's structure. Our findings demonstrate the highest coercivity in the multiphase configuration in a four-layered stack after complex treatment. It can be associated with the suppression of exchange coupling, due to local structural disorder or grain boundary segregation. As a result, each grain behaves as an isolated magnetic entity and undergoes magnetization reversal independently. In this case, ion irradiation, which modifies the interface quality and defect distribution, plays a decisive role in coercivity behavior. It is assumed that ion implantation of high energetic particles can cause local changes in the relative concentration of Co and Pt [21]. It has already been shown that an enhancement in the coercivity is attributed to defect clustering and CoPt phase formation [26].

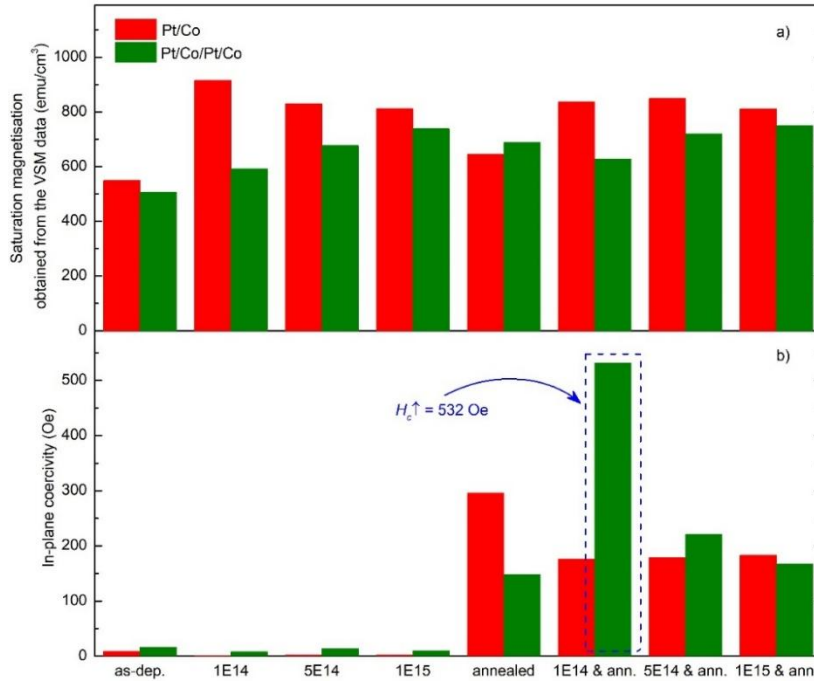


Fig. 8 – The saturation magnetization (a) and in-plane coercivity (b) of the bi-layered Pt/Co and four-layered Pt/Co/Pt/Co stacks after deposition, Ar^+ ion irradiation, single-stage annealing, and pre-irradiation followed by post-annealing

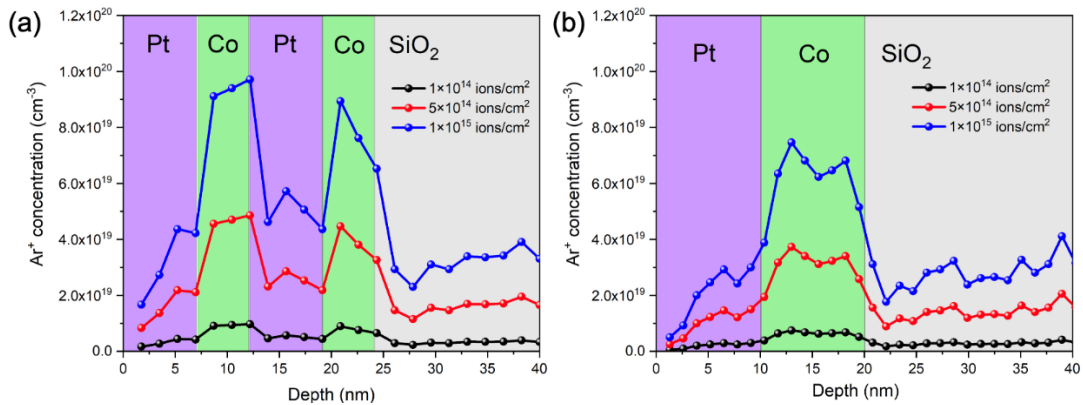


Fig. 9 – The depth distribution of the implanted Ar^+ ions of the bi-layered Pt/Co (a) and four-layered Pt/Co/Pt/Co (b) stacks as a function of fluence, obtained using SRIM simulations

In order to correlate the change in the physical properties of Pt/Co stacks due to the evolution of crystal defects under Ar⁺ ion irradiation, we performed the SRIM simulation. Figure 9 shows the simulated depth distribution of the implanted Ar⁺ ions. These results clearly show the diffusion of the Ar⁺ ions in the Pt, Co, and SiO₂ layers, in both bi-layered and four-layered stacks. There is the diffusion of the Ar⁺ ions into the Pt layer as well as the Co layer, but the concentration of implanted ions in the Pt layer is much lower. It should be noted that this diffusion is more pronounced in the case of a four-layered stack, which causes more pronounced defect generation. Moreover, a concentration gradient of Ar⁺ ions is observed across the Co/Pt interfaces. This suggests that the interfaces act as effective sinks for the accumulation and clustering of implanted ions. In this manner, these results clearly support our observation in the XRD data, where ion irradiation results in the formation of a mixture of various phases.

SRIM simulations indicate that a significant fraction of recoil events occur beyond the boundaries of the individual layers, extending into neighboring regions. This behavior implies pronounced interface roughening and enhanced atomic intermixing within the multilayer structure. Taking into account that structural analysis does not show any substantial grain growth or microstructural coarsening, the observed changes in the magnetic behavior of the four-layered stack followed by ion irradiation with fluence 1×10^{14} ions/cm², could be attributed to interface-specific atomic disordering induced by localized ion-beam effects, as was already mentioned in the work [10]. It can be concluded that choosing the optimal ion

energy and fluence can provide not only the bulk modification of magnetic properties but also the patterning of magnetic nanostructures.

4. CONCLUSIONS

In conclusion, we have investigated the modification of the structural and magnetic properties of the bi-layered Pt/Co and four-layered Pt/Co/Pt/Co stacks due to 110 keV Ar⁺ irradiations under different fluences and with subsequent thermal annealing. We observed the formation of magnetic L₁₂-CoPt₃ phase and Co/Pt solid solution during magnetron deposition processes. The following ion irradiation and thermal annealing lead to the growth of a disordered A1-CoPt phase. VSM measurements show a large coercivity of 532 Oe of preliminary irradiated and post-annealed stacks, which is indicative of a local structure disorder with Co and Pt atom displacements and defect clustering. This effect is more pronounced for the case of the four-layered stack irradiated at a fluence of 1×10^{14} ions/cm² and subjected to the following heat treatment. The obtained results offer the possibility to improve the functionality of magnetic-field sensors and spintronic devices by applying optimal conditions of ion irradiation and thermal treatment.

ACKNOWLEDGEMENTS

The work was supported by the Ministry of Education and Science of Ukraine (Projects registration numbers 0123U101257 and 0124U001266).

REFERENCES

1. C. Chappert, H. Bernas, J. Ferré, V. Kottler, J.P. Jamet, Y. Chen, H. Launois, *Science* **280** No 5371, 1919 (1998).
2. Y.N. Dong, X.N. Zhao, W. Wang, Y.X. Chen, L.H. Bai, S.S. Yan, Y.F. Tian, *J. Magn. Magn. Mater.* **559**, 169546 (2022).
3. T. Fan, N.H.D. Khang, S. Nakano, P.N. Hai, *Sci. Rep.* **12** No 1, 2998 (2022).
4. J.I. Park, S.M. Lee, S. Kim, S.J. Oh, H.C. Ri, J. Cheon, *MRS Online Proc. Libr.* **721**, E5 (2002).
5. G.S. Chang, A. Moewes, S.H. Kim, J. Lee, K. Jeong, C.N. Whang, S.C. Shin, *Appl. Phys. Lett.* **88** No 9, 092504 (2006).
6. K.A. Avchaciov, W. Ren, F. Djurabekova, K. Nordlund, I. Sveklo, A. Maziewski, *Phys. Rev. B* **92** No 10, 104109 (2015).
7. J. Jaworowicz, A. Maziewski, P. Mazalski, M. Kisielewski, I. Sveklo, M. Tekielak, J. Fassbender, *Appl. Phys. Lett.* **95** No 2, 022502 (2009).
8. E. Suharyadi, T. Kato, S. Iwata, *IEEE Trans. Magn.* **50** No 1, 3000104 (2013).
9. K. Zhang, R. Gupta, K.P. Lieb, Y. Luo, G.A. Müller, P. Schaaf, M. Uhrmacher, *Europhys. Lett.* **64** No 5, 668 (2003).
10. G. J. Kusinski, G. Thomas, *Microsc. Microanal.* **8** No 4, 319 (2002).
11. T. Blon, P. Baules, G.B. Assayag, V. Kolinský, J.C. Ousset, E. Snoeck, *J. Magn. Magn. Mater.* **315** No 1, 5 (2007).
12. P. Mazalski, Z. Kurant, A. Maziewski, M.O. Liedke, J. Fassbender, L.T. Baczewski, A. Wawro, *J. Appl. Phys.* **113** No 17, 17C109 (2013).
13. N. Sehdev, R. Medwal, R. Malik, D.C. Agarwal, K. Asokan, D. Kanjilal, S. Annapoorni, *Curr. Appl. Phys.* **14** No 3, 455 (2014).
14. J. Kim, J.W. Lee, J.R. Jeong, S.C. Shin, Y.H. Ha, Y. Park, D.W. Moon, *Phys. Rev. B* **65** No 10, 104428 (2002).
15. S. Kavita, V.R. Reddy, S. Amirthapandian, A. Gupta, B.K. Panigrahi, *J. Phys.: Condens. Matter* **21** No 9, 096003 (2009).
16. D. Ravelosona, C. Chappert, V. Mathet, H. Bernas, *J. Appl. Phys.* **87** No 9, 5771 (2000).
17. M.M. Jakubowski, M.O. Liedke, M. Butterling, E. Dynowska, I. Sveklo, E. Milińska, A. Wawro, *J. Phys.: Condens. Matter* **31** No 18, 185801 (2019).
18. C.T. Rettner, S. Anders, J.E.E. Baglin, T. Thomson, B.D. Terris, *Appl. Phys. Lett.* **80** No 2, 279 (2002).
19. M.J. Bonder, N.D. Telling, P.J. Grundy, C.A. Faunce, T. Shen, V.M. Vishnyakov, *J. Appl. Phys.* **93** No 10, 7226 (2003).
20. S. Ghosh, M. Mäder, R. Grötzschel, A. Gupta, T. Som, *Appl. Phys. Lett.* **89** No 10, 104104 (2006).
21. D. Kumar, S. Gupta, T. Jin, R. Nongjai, K. Asokan, S.N. Piramanayagam, *IEEE Magn. Lett.* **9**, 4500305 (2017).
22. A.L. Balk, K.W. Kim, D.T. Pierce, M.D. Stiles, J. Unguris, S.M. Stavis, *Phys. Rev. Lett.* **119** No 7, 077205 (2017).
23. A. Maziewski, P. Mazalski, Z. Kurant, M. O. Liedke, J. McCord, J. Fassbender, T. Gemming, *Phys. Rev. B* **85** No 5, 054427 (2012).
24. R. Pedan, I. Krulov, P. Makushko, O. Dubikovskiy, O. Kosulya, A. Orlov, I. Vladymyrskiy, *Mater. Chem. Phys.* **327**, 129862 (2024).
25. E. Lišková, M. Veis, Š. Višňovský, J. Ferré, A. Mougin, P. Mazalski, J. Fassbender, *Thin Solid Films* **520** No 24, 7169 (2012).
26. T. Som, S. Ghosh, M. Mäder, R. Grötzschel, S. Roy, D. Paramanik, A. Gupta, *New J. Phys.* **9** No 6, 164 (2007).

Підвищення коерцитивності тонких плівок Pt/Co та Pt/Co/Pt/Co шляхом іонного опромінення Ar^+ з подальшою термічною обробкою

А. Орлов¹, Р. Педань¹, І. Круглов¹, Ю. Яворський¹, О. Пальчековський¹, О. Дубіковський^{1,2},
О. Косуля², А. Боднарук^{1,3}, І. Владимирський¹

¹ Національний технічний університет України "Київський політехнічний інститут імені Ігоря Сікорського", 03056 Київ, Україна

² Інститут фізики напівпровідників імені В. Лашкарьова НАН України, 03680 Київ, Україна

³ Інститут фізики НАН України, 03028 Київ, Україна

У цій статті розглядається вплив іонного опромінення Ar^+ з подальшим термічним відпалом на магнітні та структурні властивості пліткових композицій Pt/Co та Pt/Co/Pt/Co, як функцію флюенсу іонного бомбардування. Кореляція між фазоутворенням, хімічним розподілом глибини основних компонентів і модифікацією структури, пов'язаною зі зміною коерцитивності, була досліджена за допомогою XRD, SIMS і VSM аналізу. Ми спостерігали значне збільшення коерцитивності до 532 Ое в чотиришаровій наноконструкції після попереднього іонного опромінення з флюенсом 1×10^{14} іонів/см² і подальшим відпалом при 550 °С. Спостережуване посилення коерцитивності супроводжується локальним порушенням структури зі зміщеннями атомів Co і Pt і кластеризацією дефектів, що посилюється зі збільшенням числа інтерфейсів. Ці результати добре узгоджуються з профілем глибини, оціненим незалежно за допомогою моделювання SRIM.

Ключові слова: Магнітні тонкі плівки, Іонне опромінення, Перемішування, Сплав Co-Pt, Інтерфейс, Фазоутворення.